Examining Photolysis Rates with a Prototype Online Photolysis Module in CMAQ

FRANCIS S. BINKOWSKI, SARAVANAN ARUNACHALAM, AND ZACHARIAH ADELMAN

Carolina Environmental Program, The University of North Carolina at Chapel Hill, Chapel Hill, North Carolina

JOSEPH P. PINTO

U.S. Environmental Protection Agency, Research Triangle Park, North Carolina

(Manuscript received 6 July 2006, in final form 2 October 2006)

ABSTRACT

A prototype online photolysis module has been developed for the Community Multiscale Air Quality (CMAQ) modeling system. The module calculates actinic fluxes and photolysis rates (j values) at every vertical level in each of seven wavelength intervals from 291 to 850 nm, as well as the total surface irradiance and aerosol optical depth within each interval. The module incorporates updated opacity at each time step, based on changes in local ozone, nitrogen dioxide, and particle concentrations. The module is computationally efficient and requires less than 5% more central processing unit time than using the existing CMAQ "lookup" table method for calculating j values. The main focus of the work presented here is to describe the new online module as well as to highlight the differences between the effective cross sections from the lookup-table method currently being used and the updated effective cross sections from the new online approach. Comparisons of the vertical profiles for the photolysis rates for nitrogen dioxide (NO_2) and ozone (O_3) from the new online module with those using the effective cross sections from a standard CMAQ simulation show increases in the rates of both NO_2 and O_3 photolysis.

1. Introduction

We present results from a new, efficient, online photolysis module developed for the U.S. Environmental Protection Agency's Community Multiscale Air Quality (CMAQ) modeling system (Byun and Ching 1999). This new module is designed to replace the current method of providing photolysis rates to CMAQ. Work presented here is for clear-sky conditions only. When integrated into CMAQ, the existing cloud treatment adjusts the clear-sky rates for the presence of clouds.

Photolysis rates for the current release of CMAQ, version 4.5, are provided as a lookup table generated by a program called "JPROC." This table is calculated using the delta-Eddington approach of Toon et al. (1989) and Zeng et al. (1996). Fixed profiles of ozone (O_3) and aerosol particles are used in the opacity calculation. The aerosol extinction coefficients used in CMAQ are from Elterman et al. (1969). These values are independent of time and geographic position and are representative of clean, rural background conditions. The absorption cross sections (CS) and quantum yields (QY) for ozone photolysis are not adjusted for temperature.

The lookup table contains photolysis rates for each modeled species at latitude increments of 10° (from 10° to 60°N) and values at seven altitudes with increments of 1 km from sea level to 5 km, and additional values at 10 km. All values are calculated for sea level at 1-h time intervals extending from noon to 8 h from noon; symmetry is assumed about noon. Interpolation in time and space then allocates the photolysis rates to the 3D grid of CMAQ. The tabular values from JPROC are for clear-sky conditions. Cloud adjustments of these clear-sky values are made within CMAQ during an air-quality calculation for a given episode. The use of fixed opacity profiles could generate errors in computed photolysis rates if there are sizable deviations in computed profiles of major absorbing and scattering constituents from those given in the table.

Our new online module includes the time-dependent opacity of O_3 and nitrogen dioxide (NO_2) as well as aerosol particle extinction as they develop during a

Corresponding author address: Francis S. Binkowski, UNC-Chapel Hill Carolina Environmental Program, Bank of America Plaza, 137 E. Franklin St., CB 6116, Chapel Hill, NC 27599-6116.
E-mail: frank_binkowski@unc.edu

DOI: 10.1175/JAM2531.1

TABLE 1. Effective cross sections (the product of absorption cross sections and quantum yields) for designated photolysis reactions. Values are at 298 K. Rows designated as OLM refer to the new online photolysis module, and REL rows contain the CMAQ release-version (JPROC) values; here and in Table 2, **NO_2** in boldface refers to the NO_2 to NO + $O(^3P)$ photolysis reaction, and **$O(^1D)$** in boldface refers to the O_3 to $O(^1D)$ photolysis reaction.

		Wavelength range (nm)						
Species	Method used	291.0–298.3	298.3–307.5	307.5–312.5	312.5–320.5	320.5–345.0	345.0–412.5	412.5–850.0
NO_2	OLM	9.80×10^{-20}	1.43×10^{-19}	1.85×10^{-19}	2.18×10^{-19}	3.30×10^{-19}	4.33×10^{-19}	9.59×10^{-22}
	REL	1.04×10^{-19}	1.48×10^{-19}	1.86×10^{-19}	2.22×10^{-19}	3.30×10^{-19}	4.34×10^{-19}	1.59×10^{-23}
$O(^1D)$	OLM	7.47×10^{-19}	2.49×10^{-19}	6.11×10^{-20}	1.12×10^{-20}	6.76×10^{-22}	0.00	0.00
	REL	8.82×10^{-19}	2.61×10^{-19}	5.65×10^{-20}	9.53×10^{-21}	2.59×10^{-22}	0.00	0.00

given CMAQ calculation. The new module is called for every grid cell at every synchronization time step, thereby eliminating the need for temporal and spatial interpolation. The new module calculates the solar radiative transfer in the same seven wavelength intervals used in "Fast-J," a photolysis module currently used in several global climate models (Wild et al. 2000; Bian and Prather 2002). These authors found that the seven intervals shown in Table 1 were optimal to capture the photolysis rates for O_3, NO_2, nitric acid (HNO_3), and hydrogen peroxide (H_2O_2). Six intervals were insufficient, and eight intervals added very little. Their criterion for sufficiency was an accuracy of 3%.

Absorption cross sections and quantum yields for O_3 are taken directly from Table VIII of Wild et al. (2000). For other species, the module uses values computed from the latest published values from Sander et al. (2003), the International Union of Pure and Applied Chemistry (IUPAC; online at http://www.iupac-kinetic.ch.cam.ac.uk), or from the JPROC files for each species using the algorithm presented by Wild et al. (2000) for a weighted average over each of the seven intervals. This method weights the absorption cross sections and quantum yields at each individual tabulated wavelength value within the wavelength range of each interval with the extraterrestrial solar flux at that wavelength. These individual weighted values are then summed over the range of wavelengths included in that interval and are then divided by the total extraterrestrial solar flux for that range of wavelengths. When used within CMAQ, the new updated absorption CSs and QYs are adjusted for the time-varying local temperature at the model synchronization time step. As is currently done in CMAQ, the original JPROC effective cross sections are not adjusted for temperature. Rather than showing results from CMAQ simulations using the old JPROC approach and the new online method, we will concentrate on the details of the new module.

Table 1 shows the comparison of effective cross section (absorption cross section multiplied by the quantum yield) at a temperature of 298 K. Table 2 shows the percent difference between the new and old effective cross sections. The large difference for NO_2 for interval 7 is due to the different ranges of values in the JPROC input and in the IUPAC Data Sheet PNOx4. The former has values only to a wavelength of 424 nm. The latter has values to 495 nm. For values where the wavelengths overlap, the IUPAC cross sections are larger. Thus, averaging over more and larger values produces the difference. The large differences in the values for the $O(^1D)$ oxygen atom are due to the recent reevaluations of the cross sections. Table 3 shows the effective cross sections (the product of CS and QY) for the NO_2 to nitric oxide plus oxygen atom [NO + $O(^3P)$] photolytic reaction, and Table 4 shows the effective cross sections for the O_3 to $O(^1D)$ reaction. Values are identified as being either values from the new online module ("OLM") or JPROC values from the currently released version of CMAQ ("REL"). The OLM values have been adjusted for temperature; the REL values have not been so adjusted.

In the new module, the radiative transfer calculations for the irradiances and actinic fluxes in each of the intervals are done using the efficient two-stream delta-Eddington approach (Toon et al. 1989; Zeng et al. 1996), as is also done in JPROC, but with the addition of a pseudospherical approximation from Dahlback and Stamnes (1991). This addition allows a smooth transition to low sun angles with longer slant paths.

TABLE 2. Percent differences between effective cross sections shown in Table 1. Differences are calculated from Table 1 as 100(OLM − REL)/OLM.

Bin No.	Wavelength range	Difference in **NO_2** (%)	Difference in **$O(^1D)$** (%)
1	291.0–298.3	−6.55	−18.04
2	298.3–307.5	−3.14	−5.11
3	307.5–312.5	−0.3	7.48
4	312.5–320.5	−2.21	14.61
5	320.5–345.0	−0.08	61.68
6	345.0–412.5	−0.27	0
7	412.5–850.0	98.34	0

TABLE 3. Effective cross sections (the product of absorption cross sections and quantum yields) for the NO_2 to NO + $O(^3P)$ photolytic reaction. Rows designated as OLM contain values from the new online photolysis module, and REL rows contain the CMAQ release-version (JPROC) values.

		Altitude, temperature						
Wavelength range (nm)	Method used	10 km, 236.04 K	5 km, 266.71 K	4 km, 272.49 K	3 km, 277.88 K	2 km, 282.96 K	1 km, 287.55 K	0 km, 292.13 K
291.0–298.3	OLM	9.83×10^{-20}	9.82×10^{-20}	9.81×10^{-20}	9.81×10^{-20}	9.81×10^{-20}	9.81×10^{-20}	9.80×10^{-20}
	REL	1.04×10^{-19}	1.04×10^{-19}	1.04×10^{-19}	1.04×10^{-19}	1.04×10^{-19}	1.04×10^{-19}	1.04×10^{-19}
298.3–307.5	OLM	1.43×10^{-19}	1.43×10^{-19}	1.43×10^{-19}	1.43×10^{-19}	1.43×10^{-19}	1.43×10^{-19}	1.43×10^{-19}
	REL	1.48×10^{-19}	1.48×10^{-19}	1.48×10^{-19}	1.48×10^{-19}	1.48×10^{-19}	1.48×10^{-19}	1.48×10^{-19}
307.5–312.5	OLM	1.85×10^{-19}	1.85×10^{-19}	1.85×10^{-19}	1.85×10^{-19}	1.85×10^{-19}	1.85×10^{-19}	1.85×10^{-19}
	REL	1.86×10^{-19}	1.86×10^{-19}	1.86×10^{-19}	1.86×10^{-19}	1.86×10^{-19}	1.86×10^{-19}	1.86×10^{-19}
312.5–320.5	OLM	2.18×10^{-19}	2.18×10^{-19}	2.18×10^{-19}	2.18×10^{-19}	2.18×10^{-19}	2.18×10^{-19}	2.18×10^{-19}
	REL	2.22×10^{-19}	2.22×10^{-19}	2.22×10^{-19}	2.22×10^{-19}	2.22×10^{-19}	2.22×10^{-19}	2.22×10^{-19}
320.5–345.0	OLM	3.21×10^{-19}	3.24×10^{-19}	3.25×10^{-19}	3.26×10^{-19}	3.27×10^{-19}	3.28×10^{-19}	3.28×10^{-19}
	REL	3.30×10^{-19}	3.30×10^{-19}	3.30×10^{-19}	3.30×10^{-19}	3.30×10^{-19}	3.30×10^{-19}	3.30×10^{-19}
345.0–412.5	OLM	4.23×10^{-19}	4.26×10^{-19}	4.27×10^{-19}	4.28×10^{-19}	4.29×10^{-19}	4.30×10^{-19}	4.31×10^{-19}
	REL	4.34×10^{-19}	4.34×10^{-19}	4.34×10^{-19}	4.34×10^{-19}	4.34×10^{-19}	4.34×10^{-19}	4.34×10^{-19}
412.5–850.0	OLM	8.12×10^{-22}	8.65×10^{-22}	8.81×10^{-22}	8.96×10^{-22}	9.10×10^{-22}	9.23×10^{-22}	9.36×10^{-22}
	REL	1.59×10^{-23}	1.59×10^{-23}	1.59×10^{-23}	1.59×10^{-23}	1.59×10^{-23}	1.59×10^{-23}	1.59×10^{-23}

Along with calculating photolysis rates, the new module produces aerosol optical depth (AOD) and total surface irradiance (direct + diffuse) at every surface-layer grid cell in each of the wavelength intervals. Note that total surface irradiance is output rather than actinic flux because irradiance is more appropriate than actinic flux for CMAQ applications that examine the potential effects of changes in UV radiation in response to changes in concentrations of gaseous and aerosol species.

Stratospheric ozone column amount is modeled using the method of Van Heuklon (1979). Michalsky et al. (1995) have shown that this approach might yield column amounts that are too high and may need to be scaled to a lower value, primarily as the result of stratospheric ozone depletion; this scaling would likely be dependent on location and time. For the cases presented here, we use the original Van Heuklon (1979) values.

Stevermer et al. (2000) presented information about stratospheric aerosol during background and volcanically disturbed periods. The July 2004 episode we chose for demonstrating the new photolysis module occurred during the volcanic background regime, when stratospheric AODs were at a minimum (less than 0.02). The contribution of stratospheric aerosols is therefore not considered in our calculations. The solar input reaching

TABLE 4. Effective cross sections (the product of absorption cross sections and quantum yields) for the O_3 to $O(^1D)$ photolytic reaction. Rows designated as OLM contain values from the new online photolysis module, and REL rows contain the CMAQ release-version (JPROC) values.

		Altitude, temperature						
Wavelength range (nm)	Method used	10 km, 236.04 K	5 km, 266.71 K	4 km, 272.49 K	3 km, 277.88 K	2 km, 282.96 K	1 km, 287.55 K	0 km, 292.13 K
291.0–298.3	OLM	7.02×10^{-19}	7.19×10^{-19}	7.24×10^{-19}	7.29×10^{-19}	7.33×10^{-19}	7.37×10^{-19}	7.41×10^{-19}
	REL	8.82×10^{-19}	8.82×10^{-19}	8.82×10^{-19}	8.82×10^{-19}	8.82×10^{-19}	8.82×10^{-19}	8.82×10^{-19}
298.3–307.5	OLM	2.24×10^{-19}	2.33×10^{-19}	2.36×10^{-19}	2.38×10^{-19}	2.41×10^{-19}	2.43×10^{-19}	2.45×10^{-19}
	REL	2.61×10^{-19}	2.61×10^{-19}	2.61×10^{-19}	2.61×10^{-19}	2.61×10^{-19}	2.61×10^{-19}	2.61×10^{-19}
307.5–312.5	OLM	4.57×10^{-20}	5.08×10^{-20}	5.25×10^{-20}	5.41×10^{-20}	5.57×10^{-20}	5.71×10^{-20}	5.86×10^{-20}
	REL	5.65×10^{-20}	5.65×10^{-20}	5.65×10^{-20}	5.65×10^{-20}	5.65×10^{-20}	5.65×10^{-20}	5.65×10^{-20}
312.5–320.5	OLM	5.17×10^{-21}	6.88×10^{-21}	7.57×10^{-21}	8.24×10^{-21}	8.88×10^{-21}	9.48×10^{-21}	1.01×10^{-20}
	REL	9.53×10^{-21}	9.53×10^{-21}	9.53×10^{-21}	9.53×10^{-21}	9.53×10^{-21}	9.53×10^{-21}	9.53×10^{-21}
320.5–345.0	OLM	4.28×10^{-22}	5.04×10^{-22}	5.32×10^{-22}	5.59×10^{-22}	5.85×10^{-22}	6.09×10^{-22}	6.33×10^{-22}
	REL	2.59×10^{-22}	2.59×10^{-22}	2.59×10^{-22}	2.59×10^{-22}	2.59×10^{-22}	2.59×10^{-22}	2.59×10^{-22}
345.0–412.5	OLM	0	0	0	0	0	0	0
	REL	0	0	0	0	0	0	0
412.5–850.0	OLM	0	0	0	0	0	0	0
	REL	0	0	0	0	0	0	0

the top of the CMAQ modeling domain within each wavelength interval is then diminished by passing through the model stratosphere.

A new, efficient aerosol optical code within the module is used to calculate the tropospheric aerosol optical characteristics and subsequent AOD. This code is highly optimized for the lognormal modal representation of particle size distributions used in CMAQ (Binkowski and Shankar 1995; Binkowski and Roselle 2003) as well as for the range of refractive indices of internally mixed atmospheric aerosol particles. The real and imaginary parts of the refractive indices for three particle-constituent groups (water soluble, sea salt, and dustlike) are taken from the Optical Properties of Aerosols and Clouds (OPAC) software package (Hess et al. 1998). The refractive indices for soot particles are from Table 1 of Horvath (1995). The refractive index for water is taken as 1.34, with no imaginary component (i.e., pure scattering). All values are treated as constants for all wavelengths within each particle-constituent group. The final refractive index for the internal mixture is a volume-weighted average of the individual constituent-group refractive indices. All calculations presented here are performed for clear-sky conditions—that is, attenuation of solar radiation by clouds is not considered. When integrating the new module into CMAQ, the current method of adjusting the clear-sky values for the presence of clouds is used. We realize that this method for representing clouds needs improvement by incorporation of the cloud extinction coefficients and asymmetry factors directly into the radiative transfer calculation. This will be done when funding becomes available for this purpose.

2. Presentation and discussion of results

Effects on gas phase photochemistry can perhaps best be judged by examining changes in the photolysis rates for NO_2 [referred to as "$j(NO_2)$"] and for O_3 in the Hartley bands, yielding $O(^1D)$ [referred to as "$j(O_{3Hart})$"]. This choice of metrics is supported by the work of Thompson and Stewart (1991), who found that concentrations of hydroxyl (OH) radicals are most highly correlated with these two processes.

We show results from a one-dimensional calculation using the new algorithm implemented in CMAQ. The inputs for temperature, O_3 concentrations, and aerosol extinction are from JPROC input and are representative of midlatitude summer conditions. The values for NO_2 concentrations come from Table C3 (midlatitude summer) of Thomas and Stamnes (1999). The older values from JPROC apportioned to the seven intervals using the aforementioned algorithm from Wild et al. (2000) are also implemented in the one-dimensional model to allow exact comparison of the resulting j values. To simplify the comparison with the existing CMAQ method further, the JPROC background aerosol is used in lieu of the new aerosol method designed for the CMAQ lognormal distributions. The calculation with the one-dimensional model is for noon on 29 July 2004 at 40°N.

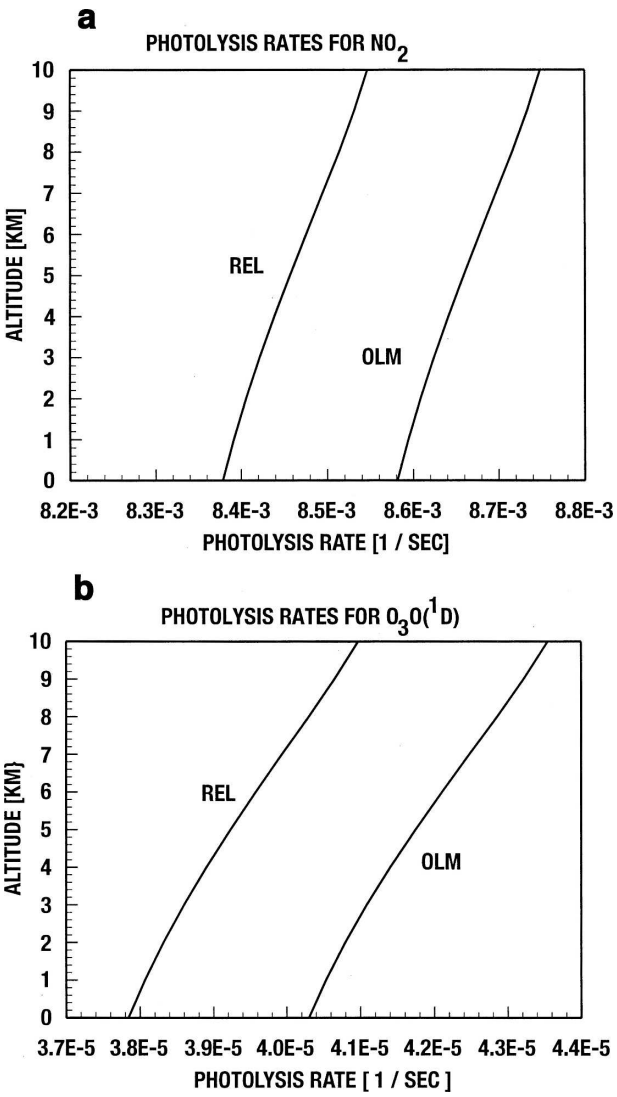

FIG. 1. Comparison of j-value profiles of (a) $j(NO_2)$ and (b) $j(O_{3Hart})$. The curves for the new online method are labeled OLM, and those for the JPROC method are labeled REL. On the x axis, the E indicates multiplication by 10 raised to the indicated power; e.g., 8.2E−3 is 8.2×10^{-3}.

Figure 1 shows vertical profiles of $j(NO_2)$ and $j(O_{3Hart})$ with the value produced using the JPROC effective cross sections, and those produced by the algorithm in the new module. The curves for the new values are labeled OLM and those using the values from JPROC are labeled REL. The only difference be-

tween the two sets of curves are the effective cross sections and the temperature adjustment performed in the OLM case. The values of $j(NO_2)$ and $j(O_{3Hart})$ for the new effective cross sections are consistently larger than the older values. The differences for $j(NO_2)$ are 2.42% at the lowest level and decrease to about 2.36% at the highest level. The differences for $j(O_{3Hart})$ are 6.50% at the lowest level and decrease to 6.28% at the highest level. Thus, the large differences in effective cross section shown in Table 2 are smoothed out somewhat by the radiative transfer calculation for the j values.

We have implemented the new online module within CMAQ with the result that central processing unit (CPU) time increased by only 5% when compared with a standard case. As noted above, the existing method of adjusting the clear-sky values for the presence of clouds in CMAQ is also applied with the new online module. We are currently performing simulations for an ozone episode that occurred in 2004 during the National Aeronautics and Space Administration (NASA) Earth Science Mission's Intercontinental Chemical Transport Experiment–North America (INTEX-NA). Details for this experiment were available on the Internet at the time of writing (http://cloud1.arc.nasa.gov/intex-na/). We will compare the results from two versions of CMAQ—CMAQ, version 4.5, as it was released to the user community in 2005 and our new version with the observations made during that experimental period. The results of these simulations and evaluations will be presented in a forthcoming journal article.

3. Summary

We have developed and implemented within CMAQ (version 4.4) a prototype method for online photolysis calculations. The new module is computationally efficient and requires less than 5% more CPU time than the existing "lookup" table for calculating j values. The new online module calculates the rates for all photolytic reactions for the release version of CMAQ at every synchronization time step and within every grid cell. Although not explicitly shown here, the new online version also produces AOD values that may then be compared with observations from satellites, as well as estimates of total surface irradiance (direct + diffuse) at every surface-layer grid cell for every wavelength interval.

Acknowledgments. This work was supported by U.S. EPA Cooperative Agreement CR-82950902-1 and NASA Grant NNG04GG29G. The authors thank our in-house reviewers, Uma Shankar and Adel Hanna, for their comments. The authors also thank two anonymous reviewers for their helpful criticism and comments.

REFERENCES

Bian, H., and M. J. Prather, 2002: Fast-J2: Accurate simulation of stratospheric photolysis in global chemical models. *J. Atmos. Chem.,* **41,** 281–296.

Binkowski, F. S., and U. Shankar, 1995: The Regional Particulate Model: Part I. Model description and preliminary results. *J. Geophys. Res.,* **100,** 26 191–26 209.

——, and S. J. Roselle, 2003: Models-3 Community Multiscale Air Quality (CMAQ) model aerosol component. 1. Model description. *J. Geophys. Res.,* **108,** 4183, doi:10.1029/2001JD001409.

Byun, D., and J. K. S. Ching, 1999: Science algorithms of the EPA Models-3 Community Multiscale Air Quality (CMAQ) modeling system. U.S. Environmental Protection Agency, Office of Research and Development Science Doc. EPA-600/R-99/030, 776 pp.

Dahlback, A., and K. Stamnes, 1991: A new spherical model for computing the radiation field available for photolysis and heating at twilight. *Planet. Space Sci.,* **39,** 671–683.

Elterman, L., R. Wexler, and D. T. Chang, 1969: Features of tropospheric and stratospheric dust. *Appl. Opt.,* **8,** 893–903.

Hess, M., P. Koepke, and I. Schult, 1998: Optical properties of aerosols and clouds: The software package OPAC. *Bull. Amer. Meteor. Soc.,* **79,** 831–844.

Horvath, H., 1995: Size segregated light absorption coefficient for the atmospheric aerosol. *Atmos. Environ.,* **29,** 875–883.

Michalsky, J. J., J. C. Liljegren, and L. C. Harrison, 1995: A comparison of sun photometer derivations of total column water vapor and ozone to standard measures of same at the Southern Great Plains Atmospheric Radiation Measurement site. *J. Geophys. Res.,* **100,** 25 995–26 003.

Sander, S. P., and Coauthors, 2003: Chemical kinetics and photochemical data for use in atmospheric studies, Evaluation Number 14. NASA Jet Propulsion Laboratory Publication 02-25, California Institute of Technology, 334 pp.

Stevermer, A., V. Petropavlovskikh, J. M. Rosen, and J. J. DeLuisi, 2000: Development of a global stratospheric climatology: Optical properties and applications for UV. *J. Geophys. Res.,* **105,** 22 763–22 776.

Thomas, G. E., and K. Stamnes, 1999: *Radiative Transfer in the Atmosphere and Ocean.* Cambridge University Press, 495 pp.

Thompson, A. M., and R. W. Stewart, 1991: Effect of chemical kinetics uncertainties on calculated constituents in a tropospheric photochemical model. *J. Geophys. Res.,* **96,** 13 089–13 108.

Toon, O. B., C. P. McKay, and T. P. Ackerman, 1989: Rapid calculation of radiative heating rates and photodissociation rates in inhomogeneous multiple scattering atmospheres. *J. Geophys. Res.,* **94,** 16 287–16 301.

Van Heuklon, T. K., 1979: Estimating atmospheric ozone for solar radiation models. *Sol. Energy,* **22,** 63–68.

Wild, O., X. Zhu, and M. J. Prather, 2000: Fast-J: Accurate simulation of in-cloud and below-cloud photolysis in tropospheric chemical models. *J. Atmos. Chem.,* **37,** 245–282.

Zeng, J., S. Madronich, and K. Stamnes, 1996: A note on the use of the two-stream delta-scaling approximation for the calculation of atmospheric photolysis rate coefficients. *J. Geophys. Res.,* **101,** 14 525–14 530.